Journal of Engineering Physics and Thermophysics, Vol. 72, No. 4, 1999

IDENTIFICATION OF THE VORTEX MECHANISM OF FRONT STABILIZATION IN MODELING OF ASYMMETRIC FLOW OF AN INCOMPRESSIBLE FLUID ALONG A CYLINDER WITH A PROTRUDING DISK

V. K. Bobyshev, S. V. Guvernyuk, and
S. A. Isaev

UDC 532.517.2

Based on numerical solution of the Navier–Stokes equations by the finite-difference method and physical modeling in a wind tunnel of laminar flow along a cylinder with a protruding disk the vortex mechanism of front stabilization and reduction in the drag of blunt bodies is investigated.

1. The concept of organizing flow along bodies by purposive formation of large-scale vortex structures in their neighborhood by placement of protruding thin plates and disks, proposed more than twenty years ago by I. A. Belov [1], proved exceptionally fruitful for attaining the positive effects of a reduction in the drag of bluff bodies and a substantial improvement of their static stability (the latter effect was named the effect of front stabilization). A composition of blunt bodies with a protruding coaxial disk made it possible to decrease their total wave resistance in the regime of supersonic flow by a factor of 2–4 [2] and to reduce the profile resistance of a cylinder by nearly two orders of magnitude [3, 4] in axisymmetric turbulent flow of an incompressible fluid along it.

The problem of reducing the resistance to the motion of bodies with organized separation of the flow as the first part of a complex problem of selecting the aerodynamic character of nontraditionally shaped bodies was solved favorably and in detail within the framework of numerical and physical modeling. Determination of the arrangements of a disk and a cylinder with considerable elongation optimum for the regime of laminar flow as far as the profile resistance and the drag are concerned [5], evaluation of the substantial effect of external turbulence [6] and compressibility [7] of the incoming flow on the resistance of bodies with a leading separation zone, extension of the idea of an organized separation of the flow to flow in a near wake behind a body, and search for the arrangement of a cylinder with little elongation and with protruding disks optimum in resistance and comparable in C_x with bodies of a streamlined shape [8] – this is by far an incomplete list of the results of systematic investigations performed on the indicated range of problems.

The problem of static stability of bodies with organized large-scale vortex structures is primarily worked through by the example of the problem of flow along loads shipped on external suspension by helicopters [9]. A technical solution of this operational problem is in selecting the suitable dimensions and the position of a baffle in front of a parallelepiped that simulates a load of the bulk or container type. But one manages to ensure the stability of flight of the bodies of this arrangement and a rather significant elongation only when tail stabilizers are used. The solution proposed was substantiated based on a complex combination of calculations, a tunnel experiment, and flight tests but the effect of front stabilization and hydrodynamic aspects of its controlling mechanism have not been adequately addressed. This is to a certain extent attributable to significant computational difficulties of solving the problem of three-dimensional flow along bodies of a nontraditional arrangement with organized separation zones. Thus, the evident shortage of information on front stabilization and the necessity of solving this problem more qualitatively and accurately dictated referring to a classical problem of flow of a viscous incompressible fluid along a semiinfinite cylinder with a disk at a nonzero angle of attack with detailing of the solution within the limits of a leading separation zone.

Academy of Civil Aviation, St. Petersburg, Russia. Translated from Inzhenerno-Fizicheskii Zhurnal, Vol. 72, No. 4, pp. 634-640, July-August, 1999. Original article submitted September 15, 1998.

 1062-0125/99/7204-0606$22.00

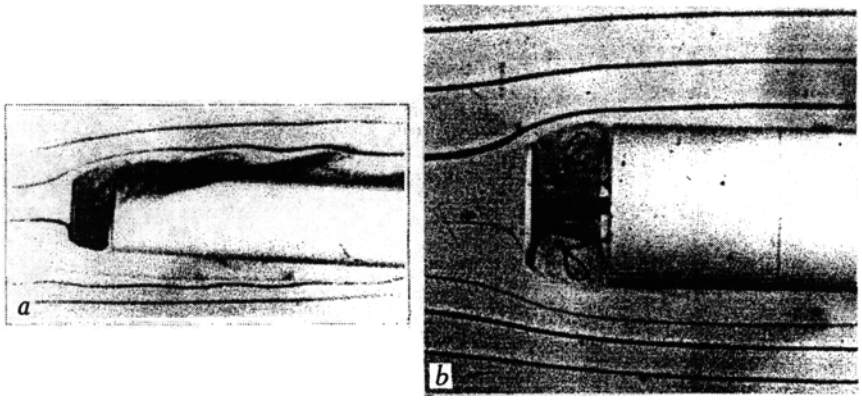

Fig. 1. Pattern of flow along a cylinder with a protruding disk with a diameter of 0.75 and a gap of 0.375 in a wind tunnel for Re = 10^3: a) $\alpha = 5^\circ$; b) $\alpha \approx 0$.

In this physical and numerical modeling, a central position is held by the detailed analysis of the controlling mechanism of front stabilization, and identification of three-dimensional jet-vortex structures by the method of computer visualization of flow based on the obtained patterns of flow spreading over the reference surfaces and observation of the tracks of tragged liquid particles with a TECPLOT package of graphic interpretation of the results of a numerical calculation is used.

2. Detached flow along models of the bodies in question is investigated experimentally in a closed-current continuous wind tunnel at low velocity ($U = 0.1$ m/sec) with a vertical test portion of $0.3 \times 0.3 \times 0.8$ m^3 volume. The radius of the model is selected from the condition of minimum occupation of the wind tunnel's test portion by the body. The thickness of the disk is 0.03. The Reynolds number of the incoming flow is 10^3. The flow velocity and the diameter of the model are selected as dimensionless scales. The flow pattern was visualized by coloring current jets with a dye (in this case, with colored ink) introduced in the flow ahead of the model from a special "comb." The model of the body fixed in a holder on the coordinate device was located in the test portion of the tunnel at different angles of attack (not exceeding $8-10^\circ$), which ensured asymmetric flow along it. Physical patterns of the flow near the bodies in question were recorded using photographic and cinematograthic equipment.

As in the case of axisymmetric flow [1], in an asymmetric case, the existence of a steady-state regime of flow along cylindrical bodies is shown, which causes the possibility of selecting a stationary mathematical model to describe it. As follows from the photographs of the patterns of detached flow along a cylinder with a protruding disk at small (of about 5°) angles of attack presented in Fig. 1 the vortex zone as a whole turns out to be localized in a gap between the disk and the cylinder similarly to the axisymmetric variant. A pronounced deformation of a large-scale vortex structure on the windward side of the cylinder end and mass removal to the lateral surface of the cylinder on the leeward side are noteworthy. In Fig. 1b, because of a small slip angle we observe well-defined vortex cores located symmetrically about the projection of a connecting rod in the pattern of return flow between the disk and the cylinder. In the computational part of the work, priority is given to analysis of the indicated hydrodynamic features of the flow in a leading separation zone (LSZ).

3. In a numerical investigation, consideration is given to the arrangement of a semiinfinite cylinder with a protruding disk ($d = 0.75$, $l = 0.375$) that is optimum in profile resistance (for high Reynolds number [3, 4]) in the regime of stable laminar flow for Re = 700 and 1000 with the formation of a leading separation zone at angles of attack of 0 and 5°. The diameter of the connecting rod is 0.18. The cylinder diameter and the velocity of the incoming flow are selected as the characteristic dimensions.

Unlike the approach developed earlier [9] on numerical modeling of detached flow along a load with the use of N-like grids that are nonorthogonal in the general case and matched with the body surface with the location of nodal points in planes perpendicular and parallel to the direction of the incoming flow with their buching near the wall and in the zones of the development of shear layers, in this investigation, we use a cylindrical grid matched with the washed surface. This enables us to substantially (by a factor of five or more) increase the density of the cells within the leading separation zone. Furthermore, to avoid problems concerned with interpolation of metric

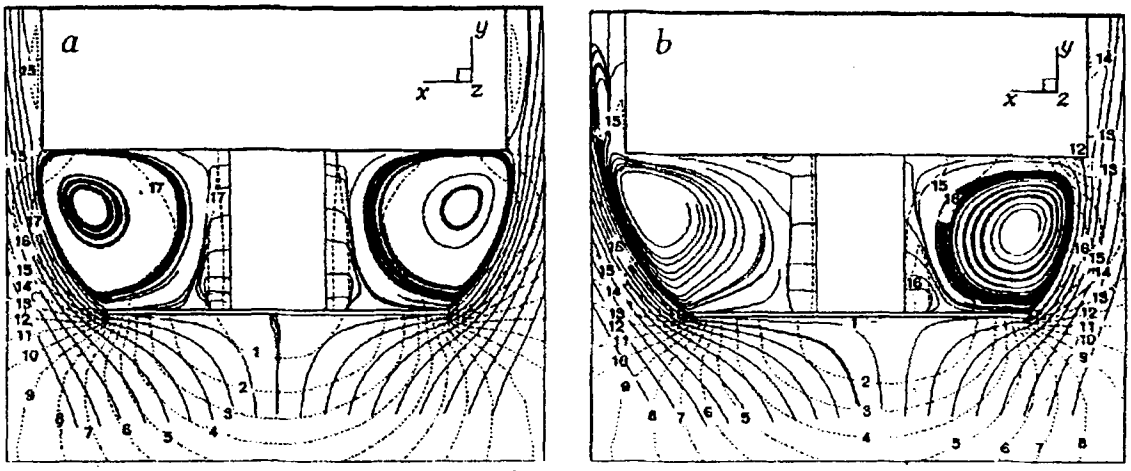

Fig. 2. Pattern of flow along a semiinfinite cylinder with a disk of diameter $d = 0.75$ and a gap $l = 0.375$ for $Re = 10^3$ in the axial plane $x - y$ at 0 (a) and 5° (b) angles of attack with the isobars drawn as dashed lines (the excess pressure is referred to the doubled velocity head): 1) $p = 0.44$; 2) 0.4; 3) 0.36; 4) 0.32; 5) 0.28; 6) 0.24; 7) 0.2; 8) 0.16; 9) 0.12; 10) 0.08; 11) 0.04; 12) 0; 13) (−0.04); 14) (−0.08); 15) (−0.12); 16) (−0.16); 17) (−0.2).

TABLE 1. Total Aerodynamic Characteristics of Compositions of Blunt Bodies and Their Components

Indices	Semiinfinite cylinder		Disk–semiinfinite cylinder arrangement for $d = 0.75$, $l = 0.375$			
Re	700		700		1000	
α	0°	5°	0°	5°	0°	5°
$C_{xc.end}$	0.762	0.779	−0.212	−0.184	−0.367	−0.293
$C_{xfr.d}$	–	–	0.42	0.42	0.378	0.367
$C_{xb.d}$	–	–	0.142	0.128	0.211	0.178
C_{xb}	0.762	0.779	0.349	0.363	0.221	0.252
$M_{zc.end}$	$-0.506 \cdot 10^{-4}$	$-0.913 \cdot 10^{-2}$	$0.183 \cdot 10^{-3}$	−0.0154	$0.176 \cdot 10^{-3}$	−0.0124
$M_{zfr.d}$	–	–	$0.28 \cdot 10^{-4}$	−0.00382	$-0.302 \cdot 10^{-4}$	−0.00495
$M_{zb.d}$	–	–	$-0.266 \cdot 10^{-4}$	0.00197	$-0.201 \cdot 10^{-4}$	$0.482 \cdot 10^{-3}$
M_{zb}	$-0.506 \cdot 10^{-4}$	$-0.913 \cdot 10^{-2}$	$-0.184 \cdot 10^{-3}$	−0.0167	$0.126 \cdot 10^{-3}$	−0.0168
V_m	−0.0606	−0.102	−0.146	−0.31	−0.192	−0.27

coefficients, we use a simplified approach based on prescribing the analytical metrics using the method of separation of variables [10]. In all the remaining details, the methodology of this investigation does not differ from the procedure of [4]. We use a tested implicit factorized algorithm for solving the Navier–Stokes equations, based on the concept of splitting by physical processes and realized in the SIMPLEC procedure of pressure correction. The initial equations in delta form for increments in dependent variables, for which natural variables – the Cartesian components of velocity and pressure – are selected, are written in arbitrary curvilinear coordinates matched with the surface in flow. Discretization of the convective terms of the explicit side of the transport equations by Leonard's scheme enables us to minimize the influence of the effects of numerical diffusion that are very substantial when detached flows are modeled, especially for large Reynolds numbers. High computational efficiency of the computational procedure is caused by discretizing the convective terms of the implicit side of the transport equations by a counterflow scheme of a first-order approximation in combination with the introduction of additional diffusion and by employing Buleev's method of incomplete matrix factorization in the Stone variant of an SIP procedure. These measures additionally ensure solution without false oscillations (monotonization of the solution). We select a centered computational pattern, i.e., all the dependent variables are determined at the center of a computational

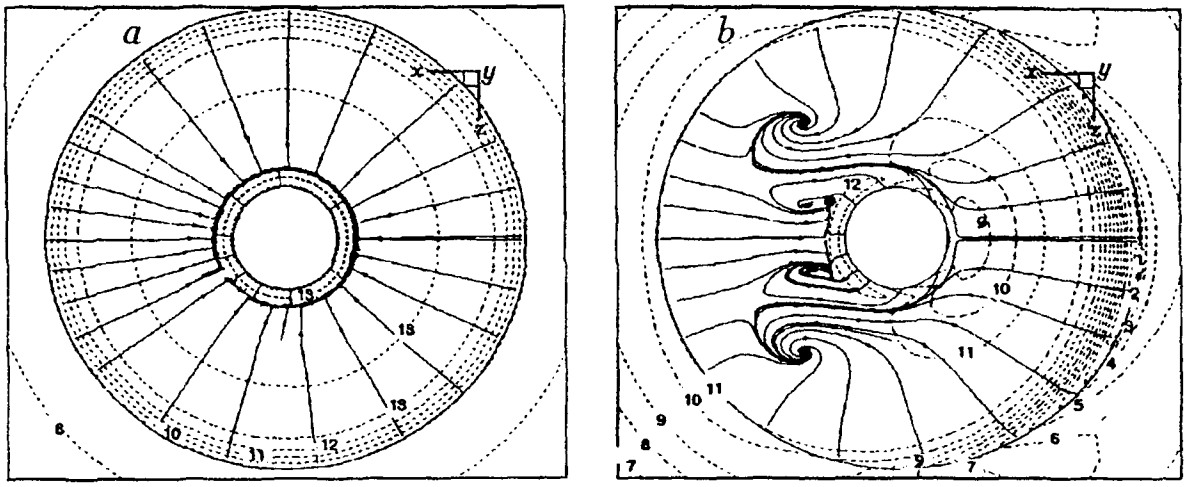

Fig. 3. Pattern of fluid spreading over the end of a cylinder with a protruding disk (Re = 10^3) at 0 (a) and 5° (b) angles of attack with the isobars drawn as dashed lines: 1) 0.04; 2) 0.02; 3) 0; 4) (−0.02); 5) (−0.04); 6) (−0.06); 7) (−0.08); 8) (−0.1); 9) (−0.12); 10) (−0.14); 11) (−0.16); 12) (−0.18); 13) (−0.2)

cell. Therefore, to avoid false pressure oscillations, in writing the equation of pressure correction, we use the Rhee–Chou approach associated with the introduction of a monotonizer (or as indicated in some works, a regularizer) of pressure correction.

At the inlet boundary of the calculation region, a uniform flow is prescribed. At the outlet boundaries, mild boundary conditions (the conditions of continuation of solution from the internal points to the boundary of the region) are set. On solid surfaces, adhesion conditions are satisfied. Steady-state flow is calculated on a grid that contains 51 × 66 × 61 cells, about 30 thousand computational nodes being concentrated in the gap between the disk and the cylinder.

4. Figures 2-4 and Table 1 compare successively calculated results for laminar flow along a semiinfinite cylinder in the presence (R = 700 and 1000) and the absence (Re =700) of a disk in front of it at angles of attack of 0 and 5°. It is pertinent to note that the results obtained are in good agreement with the data of [4, 5] on visualization of laminar detached flow in a wind tunnel and the results of calculations of two-dimensional axisymmetric flow of a cylinder with a disk.

The placement of the disk in front of the cylinder leads to a substantial rearrangement of the flow along it due to the formation of an LSZ and as a consequence to a twofold decrease in the profile resistance (C_{xb}). As Fig. 2a shows, a toroidal vortex, the intensity of the return flow (V_m) in which is 15% of the incoming-flow velocity, is realized in the gap between the disk and the cylinder at a zero angle of attack. A low (negative) pressure in the vortex that is practically the same over the entire LSZ (Fig. 3a) causes the emergence of a pull on the source side of the cylinder ($C_{xc.end}$), which predetermines the effect of the reduction in the resistance of blunt bodies with a protruding disk. The detached-flow intensity increases with Re while the profile resistance decreases substantially (by more than a factor of three as compared to C_{xb} of the cylinder).

In the presence of the angle of attack (even if comparatively small), flow along the cylinder with the disk takes on a very complex three-dimensional character. The toroidal vortex becomes deformed primarily in the axial plane parallel to the incoming flow. The vortex not only creeps to the lateral surface on the leeward side but also becomes sharply inhomogeneous. The intensification of the return flow in LSZ on the windward side (V_m increases twofold and is up to 30% of the incoming-flow velocity) is combined with strong attenuation of the detached flow on the leeward side.

The contraction of the toroidal vortex on the windward side causes a sharp pressure increase in the peripheral part of the cylinder end (Fig. 3b). On the leeward side on the end, conversely, the region of lowered pressure extends up to a sharp edge of the cylinder. As a consequence of the redistribution of local force loads

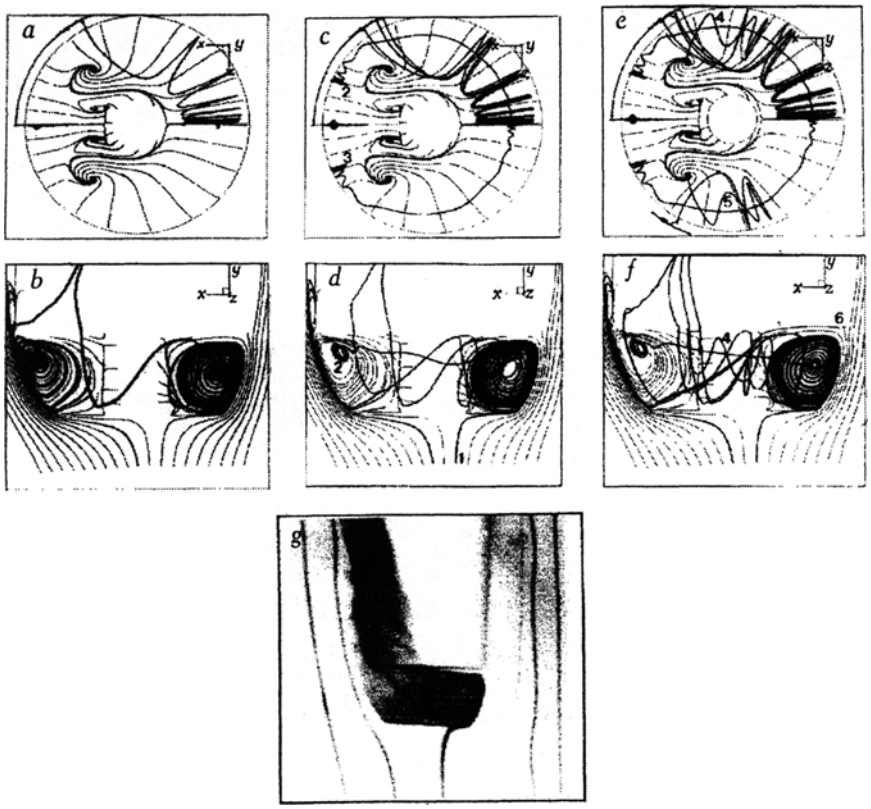

Fig. 4. Calculated tracks of liquid particles introduced at several characteristic points at the centers of the cross sections (a and b) of a large-scale vortex on the windward and leeward sides, in the incoming flow on the windward side (1) $x = -0.102$; $y = -0.606$; $z = 0.005$), in the leeward part of an LSZ (2 and 3), $x = 0.44$; $y = -0.14$; $z = \pm 0.2$), at the focuses on the leeward side of the end of a cylinder (4 and 5), $x = 0.195$; $y = -0.02$; $z = \pm 0.248$), and in the vicinity of the stagnation point in the windward part of the end (6). The patterns are presented in two projections: a view of the plane $z = 0$ (a, c, and e) and a view of the cylinder end $y = 0$ (b, d, and f); for comparison, the pattern of dyed jets of a current in the plane $z = 0$ (g) is shown.

along the end wall of the cylinder, there emerges a pair of forces that causes a significant restoring moment M_{zb} of the arrangement (the effect of front stabilization).

It is interesting to note that in flow along a cylinder without a protruding disk there is also the presence of the restoring moment induced by the separation of a flow on the lateral surface of the cylinder. However, M_{zb} turns out to be much smaller than in the case of a composition of a cylinder with a disk. As for the bodies of traditional geometry, for example, like a cylinder with a hemispherical leading part, for the arrangements of the bodies in question, their drag increases with angle of attack.

The pattern of laminar flow along the arrangement of a cylinder with a disk in question is also distinguished by the formation of the zones of secondary flow separation. However, their intensity is very low and they manifest themselves only in the regions of transition from the connecting rod to a flat end.

A complex vortex structure of flow in LSZ at a nonzero angle of attack due to strong pressure gradients is characterized by the emergence of special focus-type points of runoff on the cylinder end (Fig. 3b) when the fluid flows from the windward side to the leeward side. The flow pattern is similar to the spectrum of uniform wall flow along a cylinder installed on the plane. However, in this case, flow along the connecting rod is realized under extremely constrained conditions.

To better understand the spatial structure of jet-vortex flow, we performed its computer visualization using analysis of the behavior of tragged liquid particles introduced at different points of the space both within LSZ and

in the incoming flow. Results obtained are given successively in Fig. 4 together with a photograph of visualization of the pattern of flow along a cylinder with a disk using dyed jets in a wind tunnel.

The particles introduced at the centers of large-scale vortex structures in the plane $z = 0$ (that is parallel to the incoming flow) move along untwisting spirals, pointing to the existence of sources in the flow plane in question (Fig. 4a and b). Arriving at peripheral wall layers, one of the particles is transferred from the windward side to the leeward side with subsequent removal to the lateral surface of the cylinder, while the other particle is immediately removed from the leeward side to the lateral surface and next joins the shared jet flow there.

It is extremely interesting to observe the initiation of opposing internal jet flows in the toroidal vortices (Fig. 4c and d). Clearly their formation is caused by the inhomogeneity of the pressure field and the strong rarefaction on the windward side (Fig. 3b). In peculiar internal channels, the fluid is conveyed from the leeward side to the windward side with subsequent untwisting in the indicated plane $z = 0$ and removal of mass from LSZ onto the lateral surface. There is, in essence, an analog of a vortex tube with concentric swirling vortex counterflows. It is also pertinent to note that the fluid that arrives at LSZ from the external incoming flow flows onto the lateral surface by the scheme described above.

The special focus-type points are the sites of the concentration of sources that generate high-power tornado-like jet flows. The latter are built into the internal jet flow in LSZ that moves the fluid from the leeward zone to the windward zone. However, a very rapid untwisting of the flow in tornado structures leads to the arrival of particles at peripheral wall layers that entrain them and remove them onto the lateral surface.

Thus, at nonzero angles of attack in the case of flow along a cylinder with a protruding disk, there occurs mass supply to LSZ with the formation of complex internal jet-vortex flow and the transfer of fluid onto the lateral surface of the cylinder on its leeward part in the form of a high-power wall jet. This conclusion is confirmed by visualization of the pattern of flow along a body (Fig. 4f) that agrees well with the obtained calculated results.

The authors are thankful to G. G. Chernyi and A. I. Leont'ev for useful discussion of the problem.

The work was carried out with financial support from the Russian Fund for Basic Research (projects Nos. 98-01-00432 and 99-01-00722).

NOTATION

x, y, and z, radial, axial, and transverse Cartesian coordinates; d and l, diameter of the protruding disk and the gap between the disk and the cylinder; α, angle of attack; p, pressure; V, axial component of the velocity of return flow in LSZ; Re, Reynolds number; C_X, coefficient of resistance; M_z, lateral-torque coefficient. Subscripts: c.end, fr.d, b.d, and b refer to the cylinder end, the front of the disk, the back of the disk, and to the arrangement of the body, respectively; m, minimum.

REFERENCES

1. I. A. Belov, *Interaction of Nonuniform Flows with Obstacles* [in Russian], Leningrad (1983).
2. I. A. Belov and S. A. Isaev, *Pis'ma Zh. Tekh. Fiz.*, **6**, Issue 10, 608-611 (1980).
3. K. Koenig and A. Roshko, *J. Fluid Mech.*, **156**, 167-204 (1985).
4. I. A. Belov, S. A. Isaev, and V. A. Korobkov, *Problems and Methods of Calculation of Detached Flows of an Incompressible Fluid* [in Russian], Leningrad (1989).
5. V. K. Bobyshev, S. A. Isaev, and O. L. Lemko, *Inzh.-Fiz. Zh.*, **51**, No. 2, 224-232 (1986).
6. V. K. Bobyshev and S. A. Isaev, *Inzh.-Fiz. Zh.*, **58**, No. 4, 556-572 (1990).
7. V. K. Bobyshev and S. A. Isaev, *Inzh.-Fiz. Zh.*, **71**, No. 4, 606-612 (1998).
8. S. A. Isaev, *Inzh.-Fiz. Zh.*, **68**, No. 1, 19-25 (1995).
9. S. A. Isaev and N. A. Sumovskii, *Inzh.-Fiz. Zh.*, **70**, No. 6, 990-995 (1977).
10. S. A. Isaev, A. I. Leont'ev, A. E. Usachev, et al., "Numerical Modeling of Three-Dimensional Laminar Flow of a Viscous Incompressible Fluid About a Hole (Vortex Dynamics and Heat Transfer)" (*Preprint No. 6–97*, Institute of High-Performance Computations and Data Arrays, St. Petersburg (1997).